# JAST (Journal of Animal Science and Technology) TITLE PAGE

**Upload this completed form to website with submission**

| ARTICLE INFORMATION | Fill in information in each box below |
|---|---|
| **Article Type** | Research article |
| **Article Title (within 20 words without abbreviations)** | Fermentation-derived milk casein peptides attenuate colonic nuclear factor-kappa B signaling and associated neuroinflammatory responses in dextran sodium sulfate-induced colitis mice |
| **Running Title (within 10 words)** | Fermented casein peptides attenuate colitis and neuroinflammation |
| **Author** | Ji Seung Han[1#], Hyo Su Choi[1#], Hyun Jin Bae[1,2#], Jae Yeon Joung[1,2], Bok Kyung Han[1,3,4], Min Jae Kim[3,4], and Nam Su Oh[1*] |
| **Affiliation** | [1]Department of Food and Biotechnology, Korea University, Sejong 30019, South Korea<br>[2]Institute of Natural Science, Korea University, Sejong 30019, South Korea<br>[3]Department of Food Regulatory Science, Korea University, Sejong 30019, South Korea<br>[4]InsightFI CO., Ltd., Sejong 30019, South Korea |
| **ORCID (for more information, please visit https://orcid.org)** | Ji Seung Han (https://orcid.org/0009-0004-3569-2083)<br>Hyo Su Choi (https://orcid.org/0009-0000-5820-280X)<br>Hyun Jin Bae (https://orcid.org/0009-0001-2233-914X)<br>Jae Yeon Joung (https://orcid.org/0000-0001-6449-5004)<br>Bok Kyung Han (https://orcid.org/0000-0003-3139-0286)<br>Min Jae Kim (https://orcid.org/0009-0001-7050-6811)<br>Nam Su Oh (https://orcid.org/0000-0002-0712-7843) |
| **Competing interests** | The authors declare that there are no known competing financial interests or personal relationships that could have appeared to influence the work reported in this study. |
| **Funding sources**<br>State funding sources (grants, funding sources, equipment, and supplies). Include name and number of grant if available. | This work was supported by the National Research Foundation of Korea (NRF) grant funded by the Korean government (RS-2022-NR067505 and RS-2026-25490838). |
| **Acknowledgements** | Not applicable. |
| **Availability of data and material** | Upon reasonable request, the datasets of this study can be available from the corresponding author. |
| **Authors' contributions**<br>Please specify the authors' role using this form. | Conceptualization: Oh NS.<br>Data curation: Han JS, Choi HS, Bae HJ, Joung JY.<br>Formal analysis: Han JS, Choi HS, Bae HJ, Han BK, Kim MJ.<br>Validation: Oh NS.<br>Writing - original draft: Han JS, Choi HS, Bae HJ, Joung JY, Han BK, Kim MJ, Oh NS.<br>Writing - review & editing: Han JS, Choi HS, Bae HJ, Joung JY, Han BK, Kim MJ, Oh NS. |
| **Ethics approval and consent to participate** | All animal procedures were approved by the Institutional Animal Care and Use Committee of Korea University (KUIACUC-2025-0011). |
| **Declaration of generative AI** | No AI tools were used in this article. |

**CORRESPONDING AUTHOR CONTACT INFORMATION**

| For the corresponding author (responsible for correspondence, proofreading, and reprints) | Fill in information in each box below |
|---|---|

| | |
|---|---|
| First name, middle initial, last name | Nam Su, Oh |
| Email address – this is where your proofs will be sent | klanvin@korea.ac.kr |
| Secondary Email address | |
| Address | Department of Food and Biotechnology, Korea University, Sejong 30019, South Korea |
| Cell phone number | +82-10-2785-2907 |
| Office phone number | +82-44-860-1434 |
| Fax number | +82-44-860-1586 |

## Abstract

Fermentation of milk proteins releases bioactive peptides with potential health benefits, yet the specific peptides responsible for the anti-inflammatory activity of fermented casein remain largely unidentified. Therefore, this study aimed to identify anti-inflammatory peptides from sodium caseinate fermented with *Lactobacillus gasseri* KML39 (FSC) and to evaluate their preventive effects against colitis and colitis-associated brain alterations. FSC was fractionated, and four peptides (P1–P4) were identified from the antioxidant-active fractions by MALDI-TOF-MS/MS. Molecular docking against the TLR4/MD-2 complex was performed as an initial screening step, and all four peptides occupied the predicted binding pocket with comparable binding energies. In lipopolysaccharide (LPS)-stimulated RAW 264.7 macrophages, P1 and P4 consistently suppressed nitric oxide (NO) production and the mRNA expression of *TLR4*, *COX-2*, *iNOS*, *IL-1β*, and *IL-6*, whereas P2 and P3 showed more limited effects. Molecular dynamics simulations further showed that P1 and P4 formed more conformationally stable complexes with TLR4/MD-2 than P2 and P3, providing structural support for their selection for *in vivo* evaluation and suggesting TLR4/MD-2 as a computationally predicted target. In a dextran sodium sulfate (DSS)-induced colitis mouse model, oral pretreatment with P1 and P4 attenuated histopathological damage, suppressed NF-κB-mediated inflammatory signaling in colonic tissues, and reduced serum TNF-α levels. In the brain, both peptides reduced the pro-apoptotic marker BAX and restored the Bcl-2/BAX ratio. Notably, P4 additionally preserved intestinal barrier integrity and attenuated the colitis-associated increase in serum corticosterone, loss of blood–brain barrier Claudin-5, neuroinflammatory responses, and reduction of Bcl-2 in the brain, whereas P1 showed a narrower range of activity. Colonic inflammatory parameters were significantly correlated with serum and brain alterations. However, direct engagement of TLR4/MD-2 was not experimentally verified, the *in vivo* design assessed preventive rather than therapeutic efficacy, and the gut–brain associations were correlational. These results suggest that P4 (VLSRYPSYG), which exhibited the broadest protective profile among the identified peptides, has potential as a fermentation-derived food peptide for the preventive dietary management of intestinal inflammation and its associated neuroinflammatory consequences.



**Keywords (3 to 6)**: Peptide identification; Bioactive peptides; Fermented sodium caseinate; Molecular docking; Colitis; Neuroinflammation

# Introduction

Inflammatory bowel disease (IBD), including ulcerative colitis and Crohn's disease, is characterized by chronic inflammation of the intestinal mucosa, epithelial barrier disruption, and dysregulated immune activation [1]. Clinically, IBD manifests as diarrhea, abdominal pain, bloody stools, weight loss, and fatigue and is often accompanied by mucosal ulceration, intestinal fibrosis, and an elevated colorectal cancer risk [2]. With over seven million people affected worldwide, IBD poses a growing public health concern due to its rising prevalence and associated healthcare burden [2]. Although conventional pharmacological treatments, including 5-aminosalicylic acid and corticosteroids, alleviate symptoms, they are often associated with adverse effects and limited long-term safety, underscoring the need for safer food-derived bioactive alternatives with high tolerability and efficacy [3].

In the pathogenesis of IBD, disruption of the mucosal barrier increases intestinal permeability, facilitating microbial translocation and activation of innate immune receptors such as toll-like receptor 4 (TLR4) [1]. This cascade drives nuclear factor kappa B (NF-κB) signaling, leading to overproduction of pro-inflammatory cytokines, including tumor necrosis factor-α (TNF-α) and interleukin-6 (IL-6), which further compromise barrier integrity and perpetuate mucosal injury risk [2]. To replicate these multifaceted pathological features, dextran sodium sulfate (DSS)-induced colitis is widely used as a preclinical model of IBD. DSS disrupts the colonic epithelium, triggers microbial translocation, and activates systemic inflammatory responses, making it an ideal platform for evaluating therapeutic strategies that simultaneously target intestinal inflammatory pathways [4]. Recent studies have demonstrated that peptides derived from various dietary proteins ameliorate DSS-induced colitis through coordinated mechanisms. For example, walnut-derived peptides restored intestinal homeostasis by modulating gut microbiota composition, increasing the relative abundance of beneficial bacterial genera, such as *Prevotella* and *Akkermansia*, in colitis model mice [5].

Beyond the intestine, intestinal inflammation communicates with the brain through the neuroendocrine and immune pathways of the gut–brain axis [6]. In DSS-induced colitis, elevated circulating corticosterone and altered expression of stress-related genes in the brain have been reported [7], and colonic inflammation has been shown to induce a pro-inflammatory signature and caspase activation in the brain [8]. Circulating pro-inflammatory cytokines such as TNF-α can impair the tight junctions of the blood–brain barrier (BBB) and activate glial cells, thereby promoting neuroinflammation [9]. Accordingly, dietary interventions that attenuate colonic inflammation may also mitigate colitis-associated neuroinflammatory responses, although this possibility has not been fully explored for food-derived peptides.

Among food-derived bioactive compounds, casein-derived peptides have attracted considerable interest as multi-target, low-toxicity interventions with antioxidant and anti-inflammatory properties that protect against intestinal inflammation driven by oxidative stress and cytokine dysregulation [4, 10]. Milk-derived peptides ameliorate DSS-induced colitis by reducing inflammatory cytokine levels and disease severity in mice [11], and fermentation by lactic acid bacteria such as *Lactobacillus* species further enhances anti-inflammatory potency through improved proteolytic release of bioactive peptides, which have additionally been associated with suppression of intestinal inflammation and modulation of gut microbiota composition [10]. Because casein accounts for approximately 80% of total bovine milk protein and sodium caseinate is widely used as a dairy ingredient, identifying bioactive peptides released from fermented casein may also provide a scientific basis for the value-added utilization of dairy resources in functional food applications [12, 13].

Previous research has shown that supplementation with *Cudrania tricuspidata* leaf extract increased bacterial counts, proteolysis, and antioxidant activity during milk fermentation with *L. gasseri* strains [14, 15]. These findings provide a rationale for including the extract in the fermentation medium used to prepare sodium caseinate fermented with *Lactobacillus gasseri* KML39 (FSC). A previous study demonstrated that FSC alleviated DSS-induced colitis and associated neuroinflammation [15]; however, the specific peptides contributing to these effects had not been identified. Therefore, the present study aimed to identify the most promising anti-inflammatory peptide from FSC through a stepwise screening strategy and to evaluate its protective effects against colitis and colitis-associated brain alterations. FSC fractions were first screened based on *in vitro* antioxidant activity, and peptides were identified from the antioxidant-active fractions. The antioxidant activity of the identified peptides was subsequently evaluated directly, and molecular docking against the TLR4/MD-2 complex was performed as an initial structural screening. The peptides were then assessed for their anti-inflammatory potential in lipopolysaccharide (LPS)-stimulated RAW 264.7 macrophages, and molecular dynamics simulations were subsequently performed to evaluate the stability of peptide binding. Selected peptides were further evaluated in a DSS-induced colitis mouse model to investigate their effects on colonic NF-κB–mediated inflammatory signaling and intestinal barrier integrity, as well as on systemic stress and inflammatory responses, BBB integrity, neuroinflammation, and apoptotic signaling in the brain. In addition, correlations between colonic parameters and serum and brain parameters were analyzed to explore the association between colonic inflammation and brain alterations.

# Materials and Methods

**Preparation of fermented casein**

FSC was prepared as previously described [15]. Sodium caseinate solution was prepared by dissolving 5% (wt/wt) sodium caseinate powder (Thermo Fisher Scientific, Waltham, MA), 4.5% (wt/wt) glucose, and 0.2% (wt/wt) *Cudrania tricuspidata* leaf extract powder in distilled water. The mixture was pasteurized at 90°C for 15 min, then cooled to 37°C before inoculation with *Lactobacillus* strain. *L. gasseri* KML39 (at a concentration of $1 \times 10^6$ CFU/mL) was inoculated and incubated at 37°C for 48 h. The resulting fermented product was freeze-dried and stored at –70 °C until further use.

**Determination of proteolysis activity**

To determine proteolytic activity of FSC, fermented samples were collected at 3 h intervals. Proteolytic activity was determined using the o-phthaldialdehyde (OPA) method [16]. The FSC samples supernatants obtained by centrifugation (10,000 × g, 10 min) were mixed with OPA reagent, incubated at 37°C for 2 min, and absorbance was measured at 340 nm with Epoch 2 microplate reader (Bio-Tek Instruments Inc., Winooski, VT, USA).

**Determination of antioxidant activity**

The antioxidant activity was evaluated using the 2,2′-azino-bis (3-ethylbenzothiazoline-6-sulfonic acid) (ABTS), the 2,2-diphenyl-1-picrylhydrazyl (DPPH), and the ferric reducing antioxidant power (FRAP) assays, following the methods described by Oh et al. [17].

**Purification of casein-derived peptides using solid-phase extraction**

The peptide purification method was carried out according to Montone et al. with slight modifications [18]. The supernatant of FSC with KML39 was purified using solid-phase extraction on C18 cartridges (Bond Elut C18, 1 g, 6 mL; Agilent Technologies, Santa Clara, CA, USA). Acetonitrile was used to prepare the cartridges before adding 1 mL of the sample to each one. Then, the sample was rinsed with 15 mL of a 0.1% trifluoroacetic acid (TFA) aqueous solution. The eluted sample was collected using a mixture of acetonitrile and deionized water in a ratio of 70/30 (v/v) until the final volume reached 10 mL. After elution, the samples were concentrated using a nitrogen concentrator. Subsequently, the concentrated samples were reconstituted in 1 mL of 0.1% aqueous TFA for chromatographic purification.

**Peptide identification by HPLC and MALDI-TOF-MS**

Peptides resulting from the fermentation were separated using a preparative high-performance liquid chromatography (prep-HPLC) system equipped with an Xbridge BEH C18 OBD Prep column (19 x 250 mm, 5 μm; Waters Co., Milford, MA, USA). The mobile phase consisted of solvent A (dd$H_2O$/TFA, 99.9/0.1, v/v) and solvent B (MeOH/TFA, 99.9/0.1, v/v) at a flow rate of 17 mL/min, with a gradient of 25% solvent B (1 min) to 50% solvent B (19 min) to 95% solvent B (5 min), followed by 6 min re-equilibration. A total of 15 fractions were collected every 2 min. Subsequently, each prep-HPLC fraction was analyzed by matrix-assisted laser desorption/ionization time-of-flight tandem mass spectrometry (MALDI-TOF-MS/MS) using a previously described method [17]. Briefly, each fraction was mixed with a matrix solution, and the resulting mixture was applied to a MALDI target. The Bruker Autoflex equipment (Bruker Daltonics, Bremen, Germany) with a nitrogen laser (337 nm) was used for MALDI-TOF-MS investigations. Positive ions generated by laser desorption were accelerated at 19 kV and analyzed in reflector mode. For each mass spectrum presented, a minimum of 2000 laser shots were collected from different positions on the spots. The sequences of the identified peptides are listed in Supplementary Table S1.

The peptides used in the subsequent experiments were custom-synthesized by GenScript and supplied as lyophilized acetate salts. For the *in vitro* experiments, P1–P4 were obtained using a ≥90% purity specification; analytical HPLC of the supplied lots showed purities of 96.2% for P1, 98.1% for P2, 97.3% for P3, and 95.8% for P4. Peptide identity was verified by ESI-MS based on agreement between the theoretical and observed molecular weights. For the animal experiment, higher-purity (>95%) preparations of P1 and P4 were used. The peptides were stored at −20°C until use.

**Molecular docking**

Molecular docking simulations were performed against the TLR4/MD-2 complex (PDB ID: 2Z64; RCSB Protein Data Bank; https://www.rcsb.org/), the primary receptor responsible for LPS recognition and downstream NF-κB activation. The receptor structure was analyzed using Pharmaco-Net (Calici Co., Ltd., Seoul, Korea) to identify a peptide-binding pocket (grid box: X = −28.8259, Y = −14.1089, Z = 20.0353) using the PocketFinder™ module. Each peptide sequence was docked into this pocket using the Peptide Dock module, and binding energies (Rosetta Energy Units, REU) were calculated using DeepCalici-Plus™.

**Cell Culture**

RAW 264.7 macrophages were purchased from ATCC (Manassas, VA, USA) and cultured in Dulbecco's Modified Eagle's Medium (Gibco, Thermo Fisher Scientific, Waltham, MA, USA) supplemented with 10% fetal bovine serum (Gibco) and 1% penicillin-streptomycin (Gibco) at 37 °C in a humidified incubator with 5% $CO_2$. Cells were subcultured every 2 days when they reached 80–90% confluence.

**Cell Viability Assay**

Cytotoxicity was assessed using the 3-(4,5-dimethylthiazol-2-yl)-2,5-diphenyltetrazolium bromide (MTT) assay as previously described by Choi et al. [15] with minor modifications. Briefly, RAW 264.7 macrophage cells ($1 \times 10^4$ cells/well) were seeded in 96-well plates, pretreated with each peptide at 1 μg/mL for 12 h, and stimulated with LPS (1 μg/mL) for 18 h. 100 μL of MTT solution (5 mg/mL) was added, and after 2 h of incubation at 37 °C, formazan crystals were dissolved in dimethyl sulfoxide and the absorbance was measured at 540 nm with a microplate reader, and cell viability was calculated relative to the untreated control.

**Nitric oxide (NO) production assay**

NO production was measured using the Griess assay as previously described by Joung et al. with slight modification [19]. Briefly, RAW 264.7 cells ($1 \times 10^5$ cells/well) were seeded in 24-well plates, pretreated with peptides (1 μg/mL) for 12 h and stimulated with LPS (1 μg/mL) for 18 h. Subsequently, culture supernatants were mixed with Griess reagent, and absorbance was read at 540 nm using a microplate reader, and NO production was calculated from a sodium nitrite standard curve.

**Quantitative real-time PCR (qRT-PCR) analysis of mRNA expression**

qRT-PCR was performed as previously described [20]. Total RNA was extracted using TRIzol™ reagent (Invitrogen, Carlsbad, CA, USA) and reverse-transcribed using the BioFACT™ 2X Reverse Transcription Pre-Mix (BioFACT, South Korea). qRT-PCR was performed with GoTaq qPCR Master Mix (Promega, Madison, USA) on a QuantStudio™ 3 Real-Time PCR System (Applied Biosystems, Carlsbad, USA). Primer sequences are listed in Supplementary Table S2. Relative expression levels were calculated by the $2^{-\Delta\Delta CT}$ method [21], with *GAPDH* as a housekeeping gene.

**Molecular dynamics simulation**

MD simulations were performed using GROMACS 2026.0 to evaluate the stability of peptide binding within the TLR4/MD-2 complex. The CHARMM36m force field and TIP3P water model were applied to all systems. Each peptide–TLR4/MD-2 complex was placed in a dodecahedral periodic box with a minimum distance of 1.2 nm from the protein surface, solvated with explicit water molecules, and neutralized with $Na^+$ and $Cl^-$ ions to achieve a final salt concentration of 0.15 M. Energy minimization was performed using the steepest descent algorithm, followed by NVT equilibration at 300 K for 100 ps and NPT equilibration at 1 bar for 100 ps. Production MD simulations were subsequently conducted for 100 ns under periodic boundary conditions with an integration timestep of 2 fs (1 fs for the P3 complex, adjusted to maintain simulation stability given its initial docked geometry). Temperature and pressure were maintained using the V-rescale thermostat and Parrinello–Rahman barostat, respectively. Long-range electrostatic interactions were calculated using the Particle Mesh Ewald (PME) method with a real-space cutoff of 1.0 nm.

For each peptide–receptor complex, three independent replicate simulations (n = 3) were performed with different randomly generated initial atomic velocities at the NVT equilibration stage, while all other parameters were kept identical. Trajectory analyses were performed using GROMACS analysis tools to evaluate the structural stability of the peptide–TLR4/MD-2 complexes. Root mean square fluctuation (RMSF), backbone root mean square deviation (RMSD), radius of gyration (Rg), solvent-accessible surface area (SASA), and intermolecular hydrogen bonds were calculated, and average values for quantitative comparison were obtained from the final 50 ns of each trajectory for RMSD, Rg, and SASA, from the full 100 ns for hydrogen-bond counts, and from the MD-2 domain (residues 599–734) for RMSF. Values across the three replicates are reported as mean ± standard deviation (SD).

**Animal experiments**

Six-week-old male C57BL/6 mice were obtained from SAMTAKO (Gyeonggi-do, South Korea) and housed in a pathogen-free facility under controlled conditions (12 h light/dark cycle, 55 ± 5% relative humidity). Mice had ad libitum access to distilled water and a commercial basal diet (Envigo 2018, Doo Yeol Biotech, Seoul, South Korea). All experimental procedures were approved by the Institutional Animal Care and Use Committee of Korea University (KUIACUC-2025-0011) and conducted in accordance with IACUC guidelines. To evaluate the preventive effects of peptides against DSS-induced colitis, mice were randomly divided into four groups (n = 10 per group; three cages per group, three to four mice per cage). The control group (CON) received distilled water and

oral saline, while the DSS-treated group (NC) was given 3% (w/v) DSS in drinking water along with oral saline. The remaining two groups received 3% DSS in combination with either Peptide 1 (P1) or Peptide 4 (P4), each administered orally at a dose of 20 mg/kg of body weight per day. This dose was consistent with that used in a previous study evaluating the anti-inflammatory effects of casein-derived peptides in a DSS-induced colitis mouse model [11] and was used to assess the preventive efficacy of the purified peptides rather than to simulate their intake through conventional fermented dairy consumption. Mice received oral pretreatment with the respective peptides or saline for 10 days, followed by 3% (w/v) DSS administration in drinking water for 7 days to induce acute colitis. Body weight and clinical symptoms were recorded daily. Disease severity was evaluated using the Disease Activity Index (DAI), which integrates weight loss, stool consistency, and rectal bleeding, as previously described [22]. On day 17, all mice were euthanized and samples including blood and colon and brain tissues were collected. Colon length was measured in nine per group; one mouse per group was excluded because the colon was physically damaged during dissection, which precluded accurate measurement. The remaining colon and other tissues were allocated for downstream analyses according to a plan set before sample collection. Because Western blot, qRT-PCR, and enzyme-linked immunosorbent assay (ELISA) each required a set amount of colon and brain tissue or serum, and the same tissue could not be used for both these assays and histology, six mice per group were pre-selected for Western blot, qRT-PCR, and ELISA.

**Histopathological analysis**

Histopathological analysis was performed as previously described [15]. Briefly, colon tissues were fixed in 4% paraformaldehyde, embedded in paraffin, and sectioned at a thickness of 5 μm. The sections were stained with hematoxylin and eosin (H&E) following standard histological procedures. After staining, the sections were examined under a light microscope (Leica ICC50 E, Wetzlar, Germany) at 200× magnification, and representative images were captured for analysis. Histopathological damage was evaluated based on three parameters: severity of inflammation, depth of injury, and crypt damage. The scores for the three parameters were summed to obtain the total histopathological score, with higher scores indicating more severe colonic damage.

**Western blot analysis**

Western blotting was performed as previously described [23]. Briefly, protein concentrations were determined using a BCA assay kit (Thermo Fisher Scientific), and equal amounts (10 μg per lane) were separated by SDS-

PAGE, transferred to PVDF membranes, and probed with primary and HRP-conjugated secondary antibodies (Supplementary Table S3). Signals were detected using ECL reagent (Bio-Rad Laboratories, Hercules, CA, USA) and imaged with the iBright 750 system (Thermo Fisher Scientific). Band densities were quantified using ImageJ software (National Institutes of Health, Bethesda, MD, USA).

**Enzyme-linked immunosorbent assay (ELISA)**

Blood samples from each group were centrifuged at 4,000 × g for 10 min at 4°C to obtain serum, which was aliquoted and stored at −80°C until analysis. Serum TNF-α levels were determined using an ELISA kit (BioLegend, San Diego, CA, USA) according to the manufacturer's instructions. Serum corticosterone concentration was quantified with commercial ELISA kits (Novus Biologicals, Centennial, CO, USA) following the respective assay procedures.

**Correlation analysis**

To evaluate the associations between colonic inflammatory parameters and systemic and neuroinflammatory responses, Spearman's rank correlation analysis was performed. Fourteen colonic parameters were included: DAI, colon length, histological score, p-NF-κB/NF-κB, p-IκBα/IκBα, COX-2 and iNOS protein expression, TNF-α, COX-2 and iNOS mRNA expression, IL-1β, IL-6, Occludin, and Claudin-5. These were correlated with serum TNF-α and corticosterone levels and with twelve brain parameters: Occludin, Claudin-5, p-IκBα/IκBα, COX-2 and iNOS protein expression, TNF-α, COX-2 and iNOS mRNA expression, BAX, Bcl-2, the Bcl-2/BAX ratio, and caspase-3. Data from all experimental groups (CON, NC, P1, and P4; n = 6 per group, total n = 24) were pooled for the analysis. Spearman's correlation coefficients (ρ) and the corresponding p-values were calculated using SciPy (version 1.16.1) in Python (version 3.13), and the correlation matrix was visualized as a heatmap using Matplotlib (version 3.11.2). Statistical significance was denoted as $*p < 0.05$, $**p < 0.01$, and $***p < 0.001$.

**Statistical Analysis**

All statistical analyses were performed using GraphPad Prism software (version 10.3; GraphPad Software, San Diego, CA, USA). Results are expressed as mean ± SD. Comparisons between two groups were performed using independent-sample t-tests. Differences among groups in the RAW 264.7 cell experiments, direct peptide antioxidant assays, and single-time-point animal endpoints were evaluated by one-way analysis of variance

(ANOVA) followed by Šídák's multiple-comparison test. For qRT-PCR data, relative expression values calculated using the $2^{-\Delta\Delta Ct}$ method were log2-transformed before statistical testing, while $2^{-\Delta\Delta Ct}$ values are presented in the figures. Normality and homogeneity of variance were assessed using the Shapiro–Wilk and Brown–Forsythe tests, respectively. Statistical significance was considered at $p < 0.05$. For molecular dynamics simulation data, differences among the four peptides were evaluated using one-way ANOVA followed by Tukey's honestly significant difference (HSD) post-hoc test in Python (SciPy version 1.16.1), with significance defined as $p < 0.05$.

# Results

## Identification of FSC-derived peptides

Fermentation of sodium caseinate with KML39 significantly increased proteolytic activity and antioxidant capacity, as assessed by ABTS and DPPH radical scavenging and FRAP assays (Supplementary Fig. S1). Based on these antioxidant profiles, FSC was fractionated into 15 fractions (F1–F15) by preparative HPLC, and the three fractions exhibiting the highest antioxidant activity (F6, F7, and F9) were selected for peptide characterization (Fig. 1 and Supplementary Fig. S1). MALDI-TOF-MS/MS analysis of these active fractions identified four peptides: P1 (VPYPQRD) and P2 (RELEELN) derived from β-casein, P3 (RPKHPIKHQGLPQE) from α-S1-casein, and P4 (VLSRYPSYG) from κ-casein (Fig. 1 and Supplementary Table S1). Direct antioxidant evaluation of P1–P4 showed concentration-related increases in ABTS and DPPH radical scavenging activities and reducing power across the tested concentrations (Supplementary Fig. S2). At 1 mg/mL, P4 exhibited the highest ABTS radical scavenging activity and FRAP value, whereas P3 and P4 showed the highest DPPH radical scavenging activities. P1 also exhibited measurable antioxidant activity, particularly in the DPPH and FRAP assays, although its activity was lower than that of P4. Overall, P4 showed the strongest and most consistent antioxidant activity among the four peptides.

## Binding stability of FSC-derived peptides with the TLR4/MD-2 complex

To conduct an initial structural screening of the four peptides, molecular docking analysis was performed against the TLR4/MD-2 complex, the primary receptor responsible for LPS recognition (PDB ID: 2Z64; Supplementary Fig. S3A and B). The three-dimensional structures of the four peptides (P1–P4) were generated and docked into the selected binding pocket (Supplementary Fig. S3C). All four peptides occupied the predicted MD-2 binding pocket and formed hydrogen-bonding and hydrophobic interactions with surrounding residues, as illustrated by the docking poses and LigPlot interaction maps (Fig. 2). All four peptides exhibited comparable static binding energies (227.54–288.92 REU) and binding modes, indicating that docking alone was insufficient to discriminate among the candidates. Therefore, all four peptides were subjected to cell-based functional evaluation and MD simulation.

## Anti-inflammatory effects of FSC-derived peptides on LPS-stimulated RAW 264.7 cells

The cytotoxicity of all four peptides was first assessed in RAW 264.7 cells, and none of the peptides exerted cytotoxic effects at the tested concentration (Fig. 3A). LPS stimulation markedly elevated NO production compared with the CON group ($p < 0.0001$), and pretreatment with P1, P3, and P4 significantly inhibited this response ($p < 0.0001$), whereas P2 did not produce a statistically significant reduction (Fig. 3B). The mRNA expression levels of pro-inflammatory markers, including *TLR4*, *COX-2*, *iNOS*, *IL-1β*, and *IL-6*, were significantly upregulated in LPS-stimulated RAW 264.7 cells relative to the CON group ($p < 0.0001$; Fig. 3C). Pretreatment with each peptide differentially attenuated these responses. P1 ($p < 0.001$), P2 ($p < 0.05$), and P4 ($p < 0.01$) significantly suppressed *TLR4* mRNA expression, whereas P3 had no significant effect. *COX-2* mRNA expression was significantly reduced by P1 ($p < 0.05$) and P4 ($p < 0.01$), whereas *iNOS* mRNA expression was significantly reduced by P1 ($p < 0.001$), P3 ($p < 0.01$), and P4 ($p < 0.0001$). *IL-1β* mRNA expression was significantly attenuated by P1, P3, and P4 ($p < 0.001$), and *IL-6* mRNA expression was significantly reduced by P1 ($p < 0.01$) and P4 ($p < 0.05$).

Collectively, these results demonstrate that FSC-derived peptides differentially suppress LPS-induced pro-inflammatory responses in RAW 264.7 macrophages. Notably, P1 and P4 consistently inhibited NO production and the expression of all pro-inflammatory markers examined, whereas P2 and P3 exhibited more limited effects. Therefore, P2 and P3 were excluded from further *in vivo* evaluation, and subsequent experiments were performed with P1 and P4.

**Molecular dynamics simulation analysis of FSC-derived peptides binding stability with the TLR4/MD-2 complex**

To further characterize the binding stability of all four peptides within the TLR4/MD-2 complex, 100-ns MD simulations were performed in triplicate (n = 3 independent replicates per peptide; Fig. 4A–E; Supplementary Table S4). RMSF analysis showed that P1 and P4 exhibited significantly lower residue-level flexibility within the MD-2 domain than P2 and P3 (Fig. 4A). Consistently, P1 and P4 showed the lowest average RMSD values during the final 50 ns (0.451 ± 0.097 and 0.489 ± 0.080 nm, respectively), whereas P2 and P3 showed higher RMSD values (0.619 ± 0.020 and 0.653 ± 0.009 nm, respectively) (Fig. 4B); however, only P1 differed significantly from P2 and P3. P1 and P4 also showed slightly lower Rg and SASA values than P2 and P3 (Fig. 4C and D), although the differences in Rg were not statistically significant and SASA differed significantly only from that of P3. In addition, P1 and P4 formed fewer transient hydrogen bonds than P2 and P3 (Fig. 4E). Because hydrogen-bond count alone does not directly reflect binding stability, this metric was interpreted together with the other stability parameters rather than

as independent evidence. Notably, P1 and P4 did not differ significantly from each other in any of the measured parameters, indicating comparably stable binding for both peptides (Supplementary Table S4).

Taken together, although the four peptides exhibited comparable static docking energies, MD simulations showed that P1 and P4 formed more conformationally stable complexes with TLR4/MD-2 than P2 and P3, primarily on the basis of their lower RMSF and RMSD values. These results are in line with the broader anti-inflammatory activity of P1 and P4 in LPS-stimulated macrophages (Fig. 3) and provide structural support for the selection of P1 and P4 for subsequent *in vivo* evaluation.

**Preventive effects of FSC-derived peptides on DSS-induced colitis in mice**

The experimental design is illustrated in Fig. 5A. Body weight was significantly lower in the NC group than in the CON group by day 17 ($p < 0.05$); however, peptide-treated groups showed a similar degree of body weight reduction to the NC group, with no significant recovery observed (Fig. 5B). DAI scores were markedly higher in the NC group than in the CON group ($p < 0.0001$), while both peptide-treated groups showed significantly reduced DAI scores compared with the NC group ($p < 0.0001$; Fig. 5C). Colon length was significantly shorter in the NC group than in the CON group ($p < 0.0001$); among the peptide-treated groups, P4 significantly attenuated this reduction ($p < 0.05$), whereas P1 did not produce a statistically significant effect on colon length (Fig. 5D). Histological analysis revealed severe epithelial damage and crypt destruction in the NC group. In contrast, both peptide-treated groups showed markedly preserved epithelial structures, with reduced histological scores reflecting lower severity of inflammation, depth of injury, and crypt damage (Fig. 5E and F).

**Effects of FSC-derived peptides on colonic inflammatory signaling and intestinal barrier function in DSS-induced colitis mice**

DSS treatment significantly increased the p-NF-κB/NF-κB and p-IκBα/IκBα ratios, as well as COX-2 and iNOS protein expression levels in colonic tissues compared with the CON group ($p < 0.05$), consistent with activation of NF-κB signaling (Fig. 6A). Both P1 and P4 significantly reduced the p-NF-κB/NF-κB ratio ($p < 0.01$ and $p < 0.001$, respectively), the p-IκBα/IκBα ratio ($p < 0.01$), COX-2 ($p < 0.05$ and $p < 0.01$, respectively), and iNOS expression ($p < 0.01$) relative to the NC group. Consistent with the protein expression results, qRT-PCR analysis showed that DSS significantly increased the mRNA expression of *TNF-α*, *COX-2*, *iNOS*, *IL-1β*, and *IL-6* compared with the CON group (all $p < 0.0001$; Fig. 6B). P4 significantly reduced all five markers compared with

the NC group (*TNF-α*, *COX-2*, *iNOS*, and *IL-6*, $p < 0.0001$; IL-1β, $p < 0.001$). P1 significantly reduced *TNF-α*, *COX-2*, and *iNOS* expression (all $p < 0.0001$) and *IL-6* expression ($p < 0.001$), whereas the reduction in *IL-1β* did not reach statistical significance.

To evaluate intestinal barrier integrity, tight junction proteins were analyzed in colonic tissues (Fig. 6C). Claudin-5 protein expression was significantly reduced in the NC group compared with the CON group ($p < 0.0001$), whereas Occludin expression showed a decreasing trend that did not reach statistical significance ($p = 0.08$). P4 treatment significantly increased both Occludin ($p < 0.05$) and Claudin-5 expression ($p < 0.001$) compared with the NC group. In contrast, P1 did not significantly affect the expression of either tight junction protein. These findings suggest that, in addition to its anti-inflammatory effects, P4 more effectively preserves intestinal barrier integrity in DSS-induced colitis mice.

**Effects of FSC-derived peptides on systemic inflammation, blood–brain barrier integrity, neuroinflammation, and neuronal apoptotic signaling in DSS-induced colitis model mice**

To investigate colitis-associated neurological dysregulation, inflammatory markers in the serum and brain were evaluated (Fig. 7). Serum TNF-α levels were significantly elevated in the NC group relative to the CON group ($p < 0.001$) and were significantly reduced in both the P1 and P4 groups ($p < 0.05$; Fig. 7A). Serum corticosterone levels were similarly elevated in the NC group ($p < 0.0001$) and were significantly attenuated in the P4 group ($p < 0.01$), suggesting that DSS-induced colitis activated the hypothalamic–pituitary–adrenal (HPA) axis and that P4 treatment partially reversed this activation. Regarding BBB integrity, DSS treatment significantly reduced Occludin and Claudin-5 protein levels compared with the CON group ($p < 0.05$; Fig. 7B). Although both peptides showed a tendency to restore these reductions, the effects were protein-specific: P1 significantly restored DSS-induced decreases in Occludin expression ($p < 0.05$), whereas P4 significantly restored Claudin-5 levels ($p < 0.05$). In brain tissues, DSS-induced colitis significantly increased the p-IκBα/IκBα ratio ($p < 0.01$), together with COX-2 ($p < 0.01$) and iNOS ($p < 0.01$) protein levels, compared with the CON group (Fig. 7C). Peptide supplementation modulated these responses differently. P1 significantly reduced COX-2 ($p < 0.01$) and iNOS ($p < 0.05$) protein levels. P4 significantly attenuated the p-IκBα/IκBα ratio ($p < 0.01$) as well as COX-2 ($p < 0.01$) and iNOS ($p < 0.05$) protein levels. At the transcriptional level, COX-2 and iNOS mRNA expression in the brain was significantly increased in the NC group compared with the CON group ($p < 0.05$). Both P1 ($p < 0.01$) and P4 ($p < 0.05$) significantly suppressed COX-2 mRNA expression. In addition, P4 significantly decreased TNF-α mRNA

expression compared with the NC group ($p < 0.05$). In contrast, neither peptide significantly altered iNOS mRNA expression. Regarding neuronal apoptotic signaling, DSS treatment significantly increased the pro-apoptotic marker BAX in brain tissues compared with the CON group ($p < 0.0001$). Both peptides significantly attenuated BAX levels relative to the NC group ($p < 0.0001$; Fig. 7D). Conversely, the anti-apoptotic protein Bcl-2 was significantly decreased in the NC group compared with the CON group ($p < 0.0001$), and only P4 significantly restored Bcl-2 levels ($p < 0.01$). Consequently, the Bcl-2/BAX ratio, which was significantly reduced in the NC group ($p < 0.05$), was significantly restored by both P1 and P4 ($p < 0.01$). These results indicate that both peptides attenuate DSS-induced neuronal apoptotic signaling. P4 exhibited a broader protective effect by additionally preserving Bcl-2 expression.

Collectively, these findings demonstrate that FSC-derived peptides attenuated DSS-induced systemic inflammation, colitis-associated BBB dysfunction, neuroinflammation, and neuronal apoptosis-related signaling, with P1 and P4 showing distinct response profiles.

# Discussion

Oxidative stress and inflammation are mechanistically connected in the pathogenesis of IBD. LPS derived from gram-negative gut bacteria activates the TLR4/MD-2 receptor complex, triggering NF-κB nuclear translocation and downstream pro-inflammatory cytokine production; in turn, reactive oxygen species (ROS) generated during this inflammatory cascade promote IκBα degradation, thereby further amplifying NF-κB signaling and creating a self-perpetuating cycle of oxidative and inflammatory injury to the intestinal epithelium [24]. Building on a previous finding that FSC alleviates DSS-induced colitis and associated neuroinflammation by modulating inflammatory signaling and gut microbiota composition [15], the present study aimed to isolate peptides from FSC and identify the most promising bioactive candidate through a stepwise screening strategy. This strategy comprised *in silico* screening by molecular docking, validation of anti-inflammatory activity in LPS-stimulated macrophages, characterization of binding stability by MD simulation, and final efficacy evaluation in a DSS-induced colitis model, including the effects on the brain. Four casein-derived peptides (P1–P4) were identified from antioxidant FSC fractions. Notably, P3 (RPKHPIKHQGLPQE), an N-terminal fragment of α-S1-casein, corresponds to a sequence region previously associated with antimicrobial and antioxidant activity in the cheese-derived peptide literature [25], whereas P2 (RELEELN) and P4 (VLSRYPSYG), derived from β- and κ-casein, respectively, remain functionally uncharacterized. Given the mechanistic link between oxidative stress and NF-κB–mediated inflammatory signaling described above, antioxidant activity was used as a screening criterion to prioritize FSC fractions for peptide identification. Direct evaluation confirmed that the identified peptides themselves possessed measurable antioxidant activity, with P4 showing the strongest overall activity and P1 also exhibiting appreciable DPPH scavenging and reducing activity (Supplementary Fig. S2). However, because a fermentation control without *C. tricuspidata* leaf extract was not included in the present study, its specific contribution to KML39-mediated proteolysis and peptide release could not be determined. Furthermore, the antioxidant activity of the original FSC fractions cannot be attributed exclusively to the identified peptides, as extract-derived phenolic compounds and other non-peptide components may also have contributed to the observed activity.

Molecular docking against the TLR4/MD-2 complex was performed as an initial structural screening step, rather than targeting NF-κB itself, because NF-κB is an intracellular transcription factor lacking a distinct extracellular binding pocket, whereas TLR4/MD-2 is the upstream membrane receptor that directly engages LPS and initiates the signaling cascade leading to NF-κB activation [26]. All four peptides showed comparable binding

modes and binding energies, indicating that docking alone was insufficient to discriminate candidates and that functional evaluation was required.

Consistent with this need for functional evaluation, the anti-inflammatory activity of all four peptides was assessed in LPS-stimulated RAW 264.7 macrophages. P1 and P4 significantly suppressed NO production and the mRNA expression of all inflammatory markers examined, including *TLR4*, *COX-2*, *iNOS*, *IL-1β*, and *IL-6*. In contrast, P2 suppressed only *TLR4* expression without reducing NO production. P3 reduced NO production and *iNOS* and *IL-1β* expression but did not affect *TLR4*, *COX-2*, or *IL-6* expression. These transcriptional effects are consistent with reports that food-derived bioactive peptides can attenuate macrophage inflammatory responses through modulation of NF-κB-mediated transcriptional regulation [27]. Interestingly, the more consistent cellular responses of P1 and P4 broadly paralleled the MD-based stability pattern. Although static docking scores were comparable across the four peptides, MD simulations showed that P1 and P4 formed more stable, structurally equilibrated complexes than P2 and P3, reflecting the fundamental difference between the two approaches: docking evaluates a single optimized pose, whereas MD captures time-dependent conformational flexibility [28]. However, this correspondence is associative and does not establish that the cellular effects were mediated by direct peptide binding to TLR4/MD-2. Taken together, the broader agreement between the *in vitro* functional responses and the MD stability profiles supports the selection of P1 and P4 for *in vivo* evaluation while retaining TLR4/MD-2 as a computationally suggested rather than experimentally confirmed target.

In the DSS-induced colitis mouse model, administration of P1 and P4 attenuated hallmark pathological manifestations, as reflected by improvements in DAI scores and histological observations showing preserved colonic structure and reduced inflammatory infiltration, consistent with previous findings using other food-derived peptides [5]. Notably, P4 additionally attenuated colon shortening, whereas P1 did not produce a significant effect on this parameter, suggesting a degree of functional divergence between the two peptides despite their shared anti-inflammatory properties. However, the improvements in DAI and colonic pathology were not accompanied by a significant recovery of relative body weight. DAI is a composite index that incorporates body weight loss together with stool consistency and rectal bleeding; therefore, an improvement in DAI can occur even when body weight remains reduced if other clinical components are ameliorated. Likewise, colon length and histopathological findings primarily reflect local intestinal injury and may not change in parallel with overall body weight during an acute DSS challenge. Thus, the effects of P1 and P4 are interpreted as attenuation of several manifestations of colitis rather than complete recovery from DSS-induced weight loss. The DSS-induced colitis model replicates key features of human

IBD, including epithelial injury, mucosal immune activation, and barrier dysfunction [4], making it a well-suited platform for evaluating the coordinated protective effects of FSC-derived peptides against intestinal inflammation. Because peptides were administered only prior to DSS challenge, with no treatment during the induction phase, these findings should be interpreted as evidence of preventive rather than therapeutic efficacy. Whether P1 or P4 can ameliorate colitis once it is already established remains untested and represents an important direction for future work.

Given the central role of epithelial barrier disruption in IBD pathogenesis, both P1 and P4 effectively suppressed colonic NF-κB activation, consistent with reports that bioactive peptides attenuate NF-κB-driven inflammation by preventing IκBα degradation and scavenging ROS [29], whereas only P4 up-regulated Occludin and Claudin-5 expression. Since tight junction disruption facilitates translocation of luminal antigens and perpetuates local and systemic inflammatory signaling [30], this upregulation by P4 may represent a key upstream event preventing mucosal inflammatory progression and systemic immune activation [30]. Both P1 and P4 also reduced serum TNF-α levels, indicating attenuation of systemic inflammatory burden.

Intestinal inflammation engages neuroendocrine and immune pathways of the gut–brain axis, including HPA axis activation [6]. In the present study, DSS-induced colitis was accompanied by elevated serum corticosterone and TNF-α levels, loss of BBB tight junction proteins, and inflammatory and pro-apoptotic changes in the brain, which were attenuated by P1 and P4 to different extents. These observations are consistent with previous reports that DSS-induced colitis increases circulating corticosterone and alters stress-related gene expression in the brain [7], and that colonic inflammation induces a pro-inflammatory signature and caspase activation in the brain [8]. Circulating cytokines such as TNF-α can impair tight junctions of brain endothelial cells and activate glial cells, thereby linking peripheral inflammation to neuroinflammation [9]. In particular, TNF-α has been shown to disrupt Claudin-5-dependent endothelial barriers through NF-κB-dependent mechanisms [31]. This may explain why the restoration of brain Claudin-5 by P4 coincided with reduced serum TNF-α and attenuated IκBα phosphorylation in the brain. Moreover, only P4 reduced serum corticosterone and preserved Bcl-2 expression, suggesting that attenuation of HPA axis activation may contribute to its broader neuroprotective profile.

The correlation analysis further supported this colon–brain link. Colonic NF-κB activation, inflammatory mediators, and tight junction loss were significantly associated with serum corticosterone and TNF-α levels, as well as with BBB tight junction and apoptosis-related markers in the brain (Supplementary Fig. S4). The brain distribution of P1 and P4 was not assessed in this study. Therefore, these associations suggest that the brain-

protective effects of the peptides may be mediated, at least in part, indirectly through the attenuation of colonic and systemic inflammation rather than by a direct action on the brain. However, the correlations were derived from data pooled across all groups and therefore partly reflect differences between the healthy control and colitis groups. Moreover, correlation does not establish causality, so these associations should be regarded as hypothesis-generating. In addition, these extra-intestinal findings require further validation in defined brain regions and through behavioral assessments.

Collectively, P4 reversed a broader range of DSS-induced alterations than P1, spanning colonic inflammatory signaling, intestinal barrier integrity, HPA axis activation, BBB Claudin-5 expression, and Bcl-2-mediated anti-apoptotic signaling in the brain, whereas P1 showed activity largely confined to a subset of inflammatory and apoptosis-related markers. This functional divergence, despite the comparable MD-based binding stability that guided their selection, indicates that binding-based screening captured only part of their in vivo behavior. Because orally administered peptides may undergo gastrointestinal proteolysis [32], it remains unclear whether the observed protective effects were mediated by intact P1 and P4, their digestion-derived fragments, or a combination of both. Future studies involving simulated gastrointestinal digestion, followed by LC-MS/MS-based peptide characterization and evaluation of post-digestion anti-inflammatory activity, are needed to assess their digestive stability and the potential contribution of digestion-derived fragments to their biological effects. Although the *in silico* findings and the observed anti-inflammatory responses were consistent with the proposed involvement of TLR4/MD-2 signaling, direct receptor engagement was not experimentally verified. Future studies should directly test this proposed mechanism, for example through co-treatment with a TLR4 antagonist (e.g., TAK-242), direct binding assays such as surface plasmon resonance or isothermal titration calorimetry, or functional validation in TLR4-knockout macrophages. Together, these approaches would provide direct mechanistic evidence for the TLR4/MD-2-mediated pathway suggested by the present *in silico* and functional data.

In this study, four casein-derived peptides were identified from fermented sodium caseinate and screened through a stepwise approach combining molecular docking-based *in silico* screening, cell-based validation, MD simulation, and *in vivo* efficacy evaluation. Among them, P4 (VLSRYPSYG) emerged as the lead candidate through convergent computational, cellular, and *in vivo* evidence, showing the broadest preventive efficacy against DSS-induced colitis by suppressing NF-κB-mediated inflammation and preserving intestinal barrier integrity. P4 also attenuated colitis-associated systemic stress and inflammatory responses, BBB Claudin-5 loss, and neuroinflammatory and apoptotic signaling in the brain, and these brain changes were closely associated with the

severity of colonic inflammation. These findings support P4 as a promising fermentation-derived food peptide for the preventive dietary management of intestinal inflammation and its associated neuroinflammatory consequences. However, TLR4/MD-2 engagement was inferred computationally, the *in vivo* design evaluated preventive rather than therapeutic efficacy, and the gut–brain associations were correlational rather than causal. Further studies are needed to verify the TLR4/MD-2-mediated mechanism, therapeutic efficacy in established colitis, and region-specific and behavioral effects in the brain.

## CRediT authorship contribution statement

NS: Conceptualization, Validation, Writing – Original draft, Writing – Review & Editing.

JS, HS, and HJ: Data curation, Formal analysis, Writing – Original draft, Writing – Review & Editing

JY: Data curation, Writing – Original draft, Writing – Review & Editing

BK and MJ: Formal analysis, Writing – Original draft, Writing – Review & Editing.

All authors have read and approved the final manuscript.


## Funding

This work was supported by the National Research Foundation of Korea (NRF) grant funded by the Korean government (RS-2022-NR067505 and RS-2026-25490838).


## Competing interests

The authors declare that there are no known competing financial interests or personal relationships that could have appeared to influence the work reported in this study.

## Ethics approval

All animal procedures were approved by the Institutional Animal Care and Use Committee of Korea University (KUIACUC-2025-0011).

## Data availability

Upon reasonable request, the datasets of this study can be available from the corresponding author.

# References


1. Kałużna A, Olczyk P, Komosińska-Vassev K. The role of innate and adaptive immune cells in the pathogenesis and development of the inflammatory response in ulcerative colitis. Journal of clinical medicine. 2022;11(2):400.

2. Balestrieri P, Ribolsi M, Guarino MPL, Emerenziani S, Altomare A, Cicala M. Nutritional aspects in inflammatory bowel diseases. Nutrients. 2020;12(2):372.

3. Honap S, Jairath V, Danese S, Peyrin-Biroulet L. Navigating the complexities of drug development for inflammatory bowel disease. Nature Reviews Drug Discovery. 2024;23(7):546-62.

4. Qiu W, Wang Z, Liu Q, Du Q, Zeng X, Wu Z, et al. Structure and regulatory mechanisms of food-derived peptides in inflammatory bowel disease: A review. Food science & nutrition. 2024;12(9):6055-69.

5. Qi Y, Wang X, Zhang Y, Leng Y, Liu X, Wang X, et al. Walnut-Derived Peptide Improves Cognitive Impairment in Colitis Mice Induced by Dextran Sodium Sulfate via the Microbiota–Gut–Brain Axis (MGBA). Journal of Agricultural and Food Chemistry. 2023;71(49):19501-15.

6. Cryan JF, O'Riordan KJ, Cowan CS, Sandhu KV, Bastiaanssen TF, Boehme M, et al. The microbiota-gut-brain axis. Physiological reviews. 2019;99(4):1877-2013.

7. Reichmann F, Hassan AM, Farzi A, Jain P, Schuligoi R, Holzer P. Dextran sulfate sodium-induced colitis alters stress-associated behaviour and neuropeptide gene expression in the amygdala-hippocampus network of mice. Sci Rep. 2015;5:9970.

8. Talley S, Valiauga R, Anderson L, Cannon AR, Choudhry MA, Campbell EM. DSS-induced inflammation in the colon drives a proinflammatory signature in the brain that is ameliorated by prophylactic treatment with the S100A9 inhibitor paquinimod. J Neuroinflammation. 2021;18(1):263.

9. Sun Y, Koyama Y, Shimada S. Inflammation From Peripheral Organs to the Brain: How Does Systemic Inflammation Cause Neuroinflammation? Front Aging Neurosci. 2022;14:903455.

10. Saubenova M, Oleinikova Y, Rapoport A, Maksimovich S, Yermekbay Z, Khamedova E. Bioactive peptides derived from whey proteins for health and functional beverages. Fermentation. 2024;10(7):359.

11. Ha J, Oh H, Oh NS, Seo Y, Kang J, Park MH, et al. Anti-Inflammatory Effect of a Peptide Derived From the Synbiotics, Fermented Cudrania tricuspidata With Lactobacillus gasseri, on Inflammatory Bowel Disease. Mediators of Inflammation. 2020;2020(1):3572809.

12. Davoodi SH, Shahbazi R, Esmaeili S, Sohrabvandi S, Mortazavian A, Jazayeri S, et al. Health-Related Aspects of Milk Proteins. Iran J Pharm Res. 2016;15(3):573-91.

13. Zhou J, Yue S, Xue B, Wang Z, Wang L, Peng Q, et al. Enhanced supply of methionine regulates protein synthesis in bovine mammary epithelial cells under hyperthermia condition. J Anim Sci Technol. 2021;63(5):1126-41.

14. Oh NS, Lee JY, Oh S, Joung JY, Kim SG, Shin YK, et al. Improved functionality of fermented milk is mediated by the synbiotic interaction between Cudrania tricuspidata leaf extract and Lactobacillus gasseri strains. Applied Microbiology and Biotechnology. 2016;100(13):5919-32.

15. Choi HS, Joung JY, Bae HJ, Oh NS. Fermented casein with Lactobacillus gasseri KML39 alleviates systemic inflammation interacting with the gut-brain-microbiome axis in dextran sulfate sodium–induced colitis mice. Journal of Dairy Science. 2025.

16. Shori AB, Hong YC, Baba AS. Proteolytic profile, angiotensin-I converting enzyme inhibitory activity and sensory evaluation of Codonopsis pilosula and fish collagen cheese. Food Research International. 2021;143:110238.

17. Oh NS, Joung JY, Lee JY, Kim Y, Kim SH. Enhancement of antioxidative and intestinal anti-inflammatory activities of glycated milk casein after fermentation with Lactobacillus rhamnosus 4B15. Journal of agricultural and food chemistry. 2017;65(23):4744-54.

18. Montone CM, Capriotti AL, Cavaliere C, La Barbera G, Piovesana S, Chiozzi RZ, et al. Characterization of antioxidant and angiotensin-converting enzyme inhibitory peptides derived from cauliflower by-products by multidimensional liquid chromatography and bioinformatics. Journal of Functional Foods. 2018;44:40-7.

19. Joung JY, Choi K, Lee J-H, Oh NS. Protective potential of Limosilactobacillus fermentum strains and their mixture on inflammatory bowel disease via regulating gut microbiota in mice. Journal of microbiology and biotechnology. 2024;35:e2410009.

20. Kim JH, Lee WJ, Choi KY, Yoo S-H, Pack SP, Oh NS. Exopolysaccharide from Lacticaseibacillus rhamnosus IR06 as a potential postbiotics attenuates photoaging through regulation of MAPK and NF-κB signaling. Free Radical Biology and Medicine. 2025.

21. Livak KJ, Schmittgen TD. Analysis of relative gene expression data using real-time quantitative PCR and the 2− ΔΔCT method. methods. 2001;25(4):402-8.

22. Pandurangan AK, Mohebali N, Norhaizan ME, Looi CY. Gallic acid attenuates dextran sulfate sodium-induced experimental colitis in BALB/c mice. Drug design, development and therapy. 2015:3923-34.

23. Jang JH, Joung JY, Pack SP, Oh NS. Preventive effect of fermented whey protein mediated by Lactobacillus gasseri IM13 via the PI3K/AKT/FOXO pathway in muscle atrophy. Journal of Dairy Science. 2024;107(5):2606-19.

24. Morgan MJ, Liu ZG. Crosstalk of reactive oxygen species and NF-kappaB signaling. Cell Res. 2011;21(1):103-15.

25. Guha S, Sharma H, Deshwal GK, Rao PS. A comprehensive review on bioactive peptides derived from milk and milk products of minor dairy species. Food production, processing and nutrition. 2021;3(1):2.

26. Park BS, Song DH, Kim HM, Choi BS, Lee H, Lee JO. The structural basis of lipopolysaccharide recognition by the TLR4-MD-2 complex. Nature. 2009;458(7242):1191-5.

27. Zhou N, Wu N, Yao Y, Chen S, Xu M, Yin Z, et al. Anti-inflammatory effects of tripeptide WLS on TNF-α-induced HT-29 cells and DSS-induced colitis in mice. Food & Function. 2022;13(18):9496-512.

28. Hospital A, Goni JR, Orozco M, Gelpi JL. Molecular dynamics simulations: advances and applications. Adv Appl Bioinform Chem. 2015;8:37-47.

29. Liu D, Zhong Z, Karin M. NF-κB: A Double-Edged Sword Controlling Inflammation. Biomedicines. 2022;10(6):1250.

30. Heazlewood CK, Cook MC, Eri R, Price GR, Tauro SB, Taupin D, et al. Aberrant mucin assembly in mice causes endoplasmic reticulum stress and spontaneous inflammation resembling ulcerative colitis. PLoS medicine. 2008;5(3):e54.

31. Clark PR, Kim RK, Pober JS, Kluger MS. Tumor necrosis factor disrupts claudin-5 endothelial tight junction barriers in two distinct NF-kappaB-dependent phases. PLoS One. 2015;10(3):e0120075.

32. Ahmed T, Sun X, Udenigwe CC. Role of structural properties of bioactive peptides in their stability during simulated gastrointestinal digestion: A systematic review. Trends in Food Science & Technology. 2022;120:265-73.

# Tables and Figures

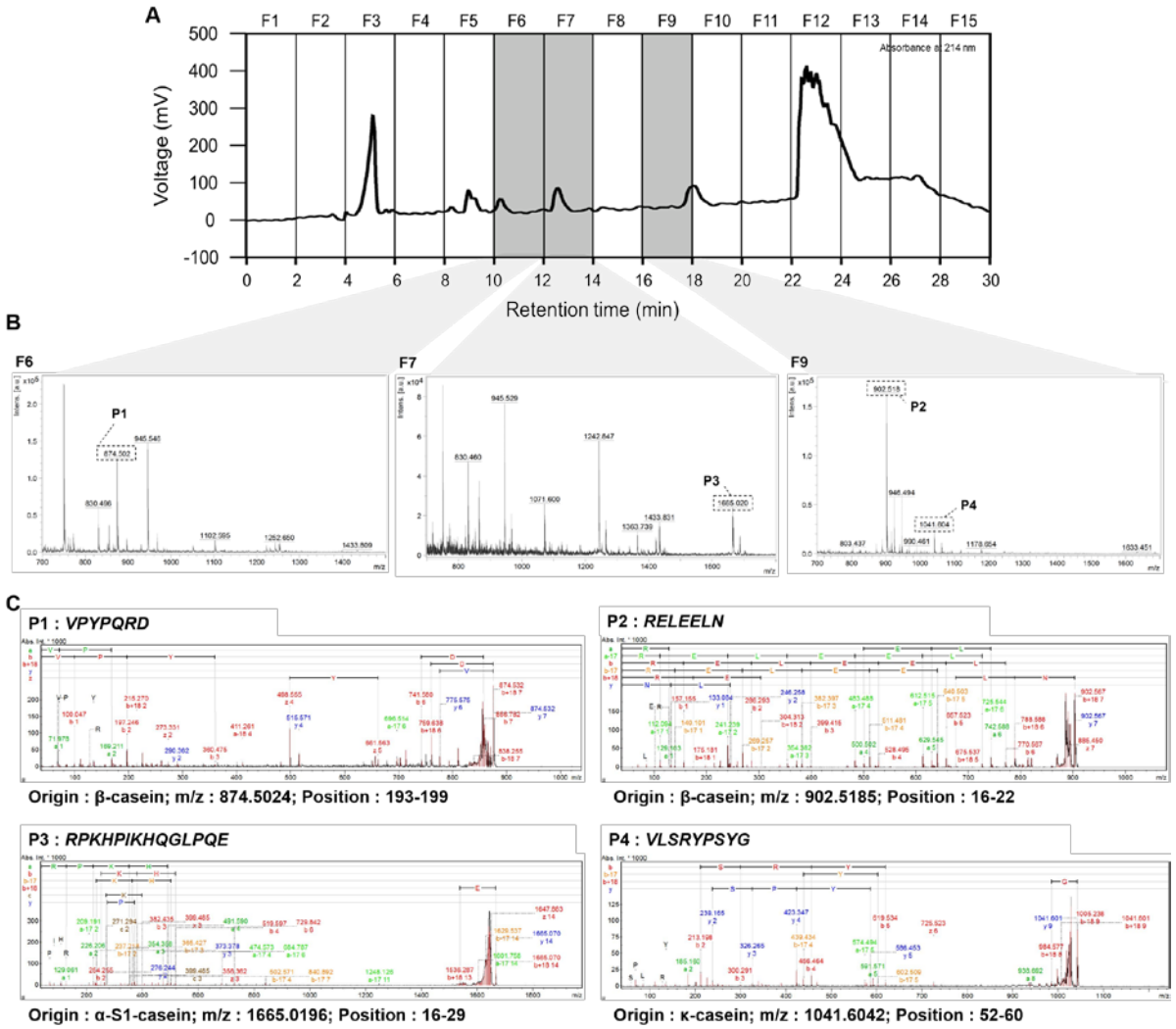
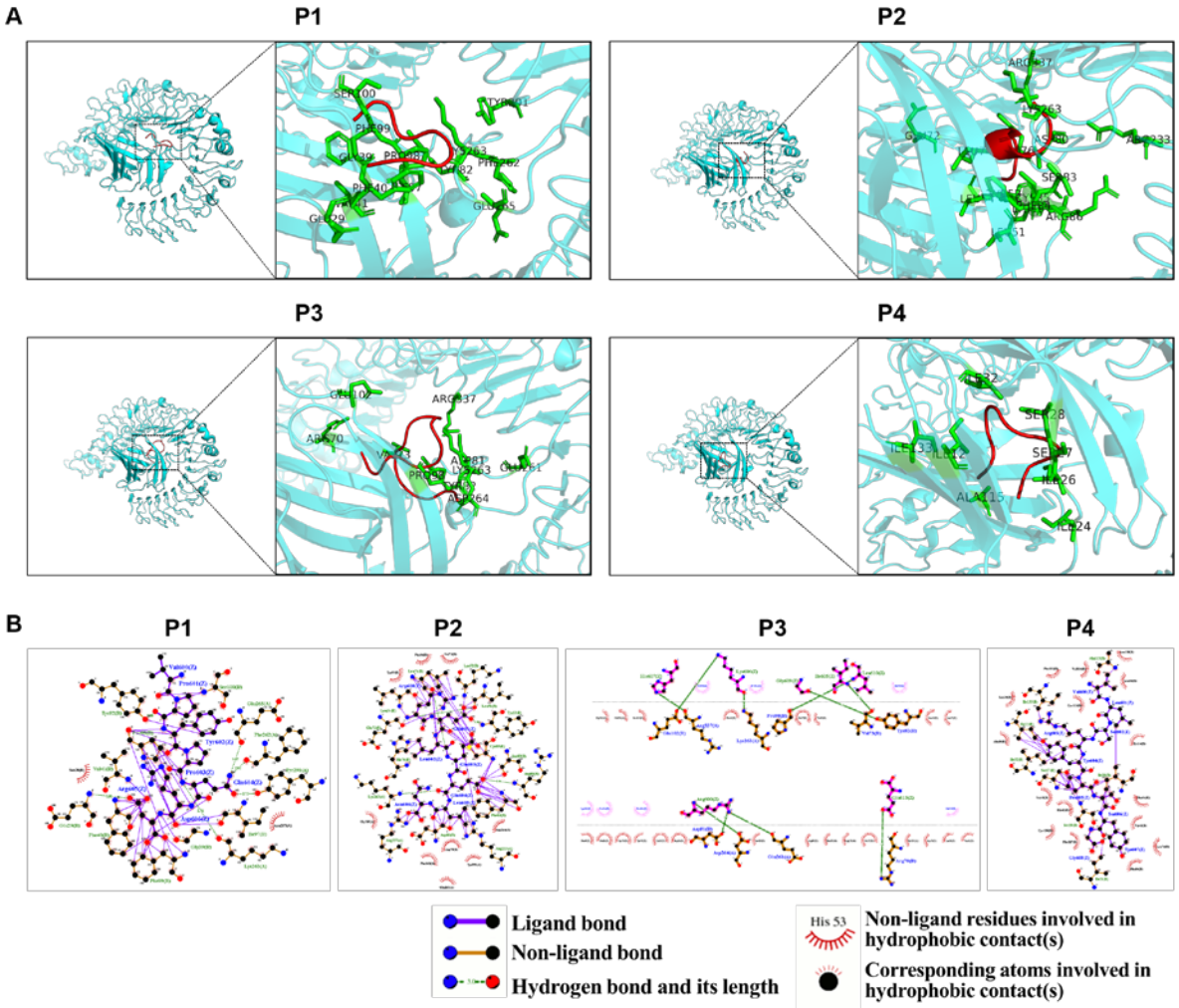



**Fig. 1 Fractionation of FSC and identification of antioxidant peptides.** (A) Preparative HPLC chromatogram of FSC showing the collection of fractions F1–F15. (B) MALDI-TOF mass spectra of antioxidant-active fractions. (C) Amino acid sequences and precursor ion information of peptides identified by MALDI-TOF-MS/MS analysis. Peptides were identified from antioxidant-active fractions F6, F7, and F9 and mapped to their corresponding parent casein proteins.




627

628 **Fig. 2 Molecular docking of FSC-derived peptides with the TLR4/MD-2 complex.** (A) Docking poses and (B)

629 LigPlot interaction maps of P1–P4 within the predicted MD-2 binding pocket.

630

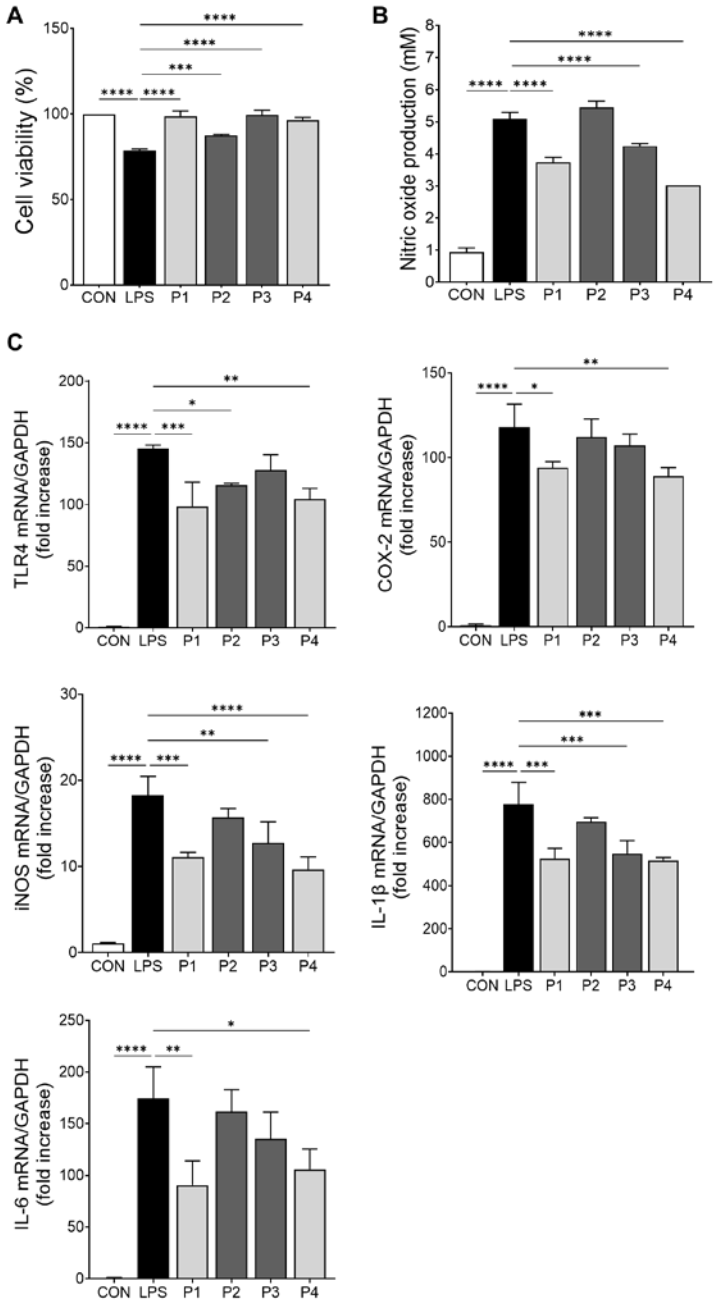



**Fig. 3 Anti-inflammatory effects of FSC-derived peptides in LPS-stimulated RAW 264.7 macrophages.** (A) Cell viability of RAW 264.7 cells treated with FSC-derived peptides (P1–P4). (B) Nitric oxide (NO) production in LPS-stimulated RAW 264.7 cells following peptide treatment. (C) Relative mRNA expression levels of inflammatory markers, including *TLR4*, *COX-2*, *iNOS*, *IL-1β*, and *IL-6*, determined by qRT-PCR. mRNA levels were normalized to *GAPDH*. Data are presented as mean ± SD (n = 3). Statistical significance was determined by one-way ANOVA followed by Šídák's multiple comparison test. *$p < 0.05$, **$p < 0.01$, ***$p < 0.001$, ****$p < 0.0001$.

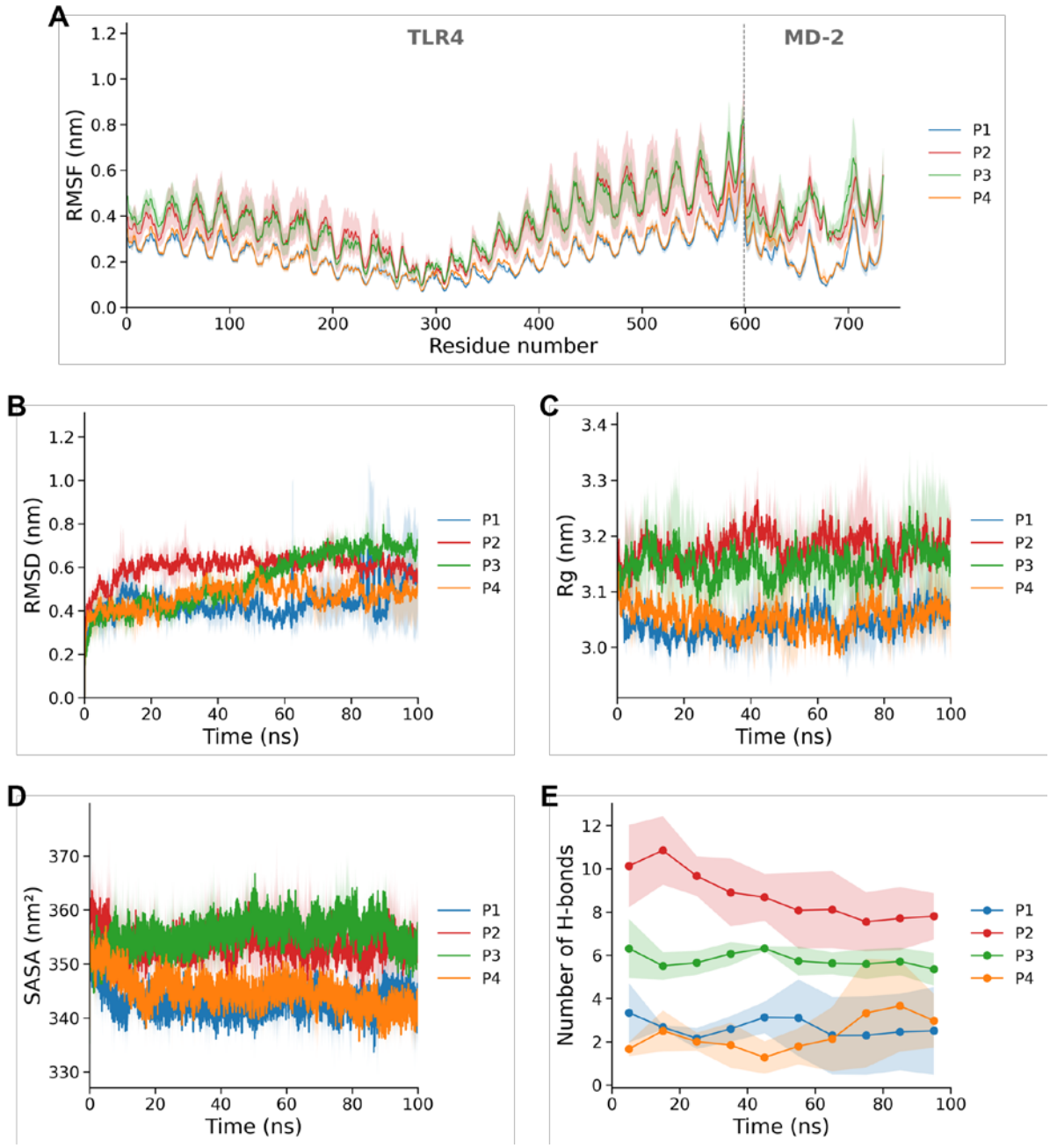



**Fig. 4 Molecular dynamics simulation analysis of FSC-derived peptides within the TLR4/MD-2 complex.** (A) RMSF profiles of TLR4/MD-2 residues. The dashed line indicates the boundary between the TLR4 and MD-2 domains. (B) Backbone RMSD profiles during 100 ns MD simulations. (C) Radius of gyration (Rg) profiles. (D) Solvent-accessible surface area (SASA) profiles. (E) Average numbers of intermolecular hydrogen bonds between the peptides and the TLR4/MD-2 complex during the simulation period. Peptides are represented as P1 (blue), P2 (red), P3 (green), and P4 (orange). In (A)–(E), solid lines represent the mean across three independent replicate simulations (n = 3), and shaded areas represent ±1 SD.

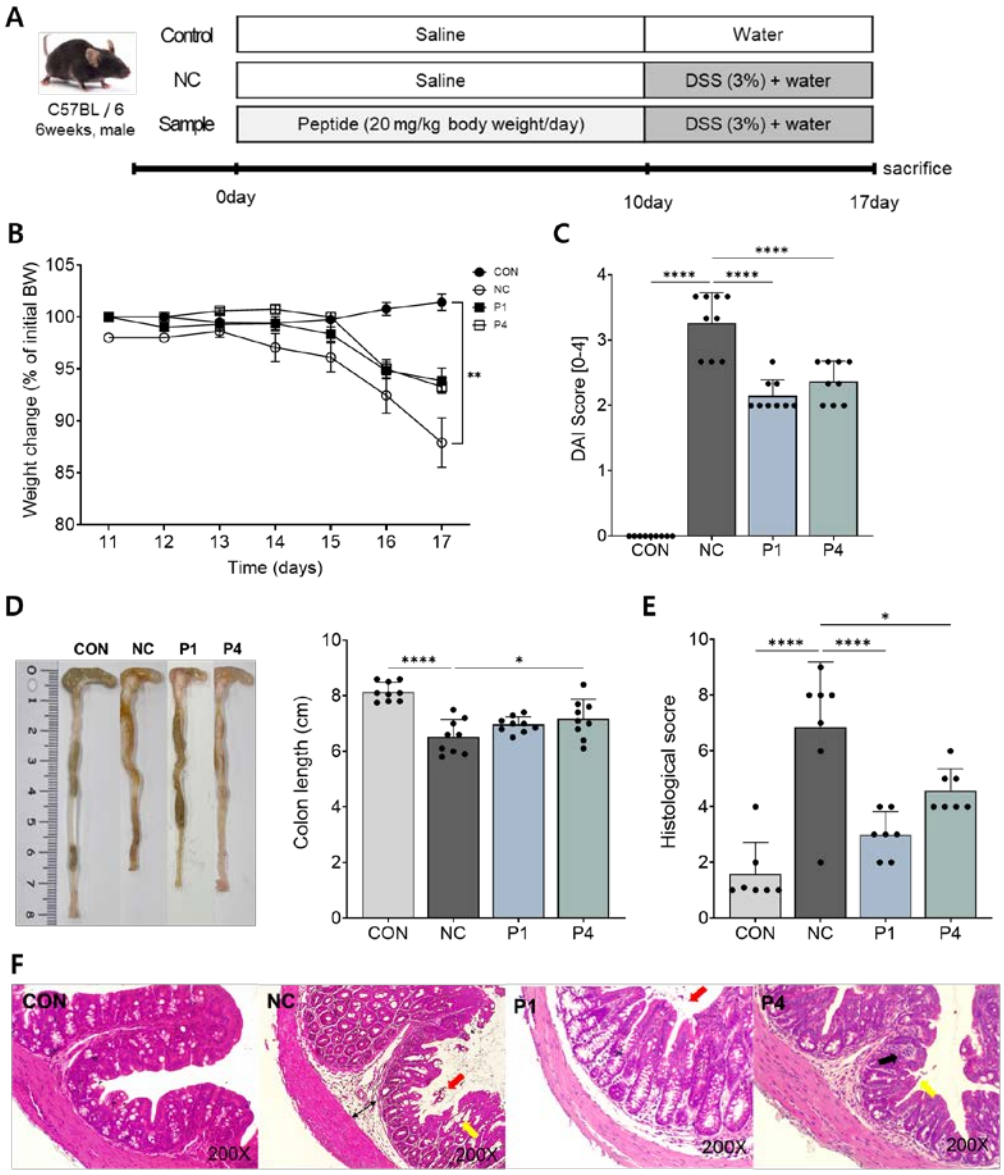



**Fig. 5 Protective effects of FSC-derived peptides against DSS-induced colitis in mice.** (A) Schematic representation of the DSS-induced colitis model and peptide administration protocol. (B) Body weight changes during the experimental period. (C) Disease activity index (DAI) scores. (D) Colon length and representative colon images (n = 9). (E) Histological scores based on inflammation severity, injury depth, and crypt damage. (F) Representative hematoxylin and eosin (H&E)-stained colonic sections (200×). Red arrows indicate epithelial damage; yellow arrows denote crypt loss and abscesses; black arrows indicate goblet cell depletion; double-headed arrows indicate submucosal thickening. For panel B, statistical comparison was performed at day 17. Statistical significance was determined by one-way ANOVA followed by Šídák's multiple comparison test. *$p < 0.05$, **$p < 0.01$, ***$p < 0.001$, ****$p < 0.0001$.

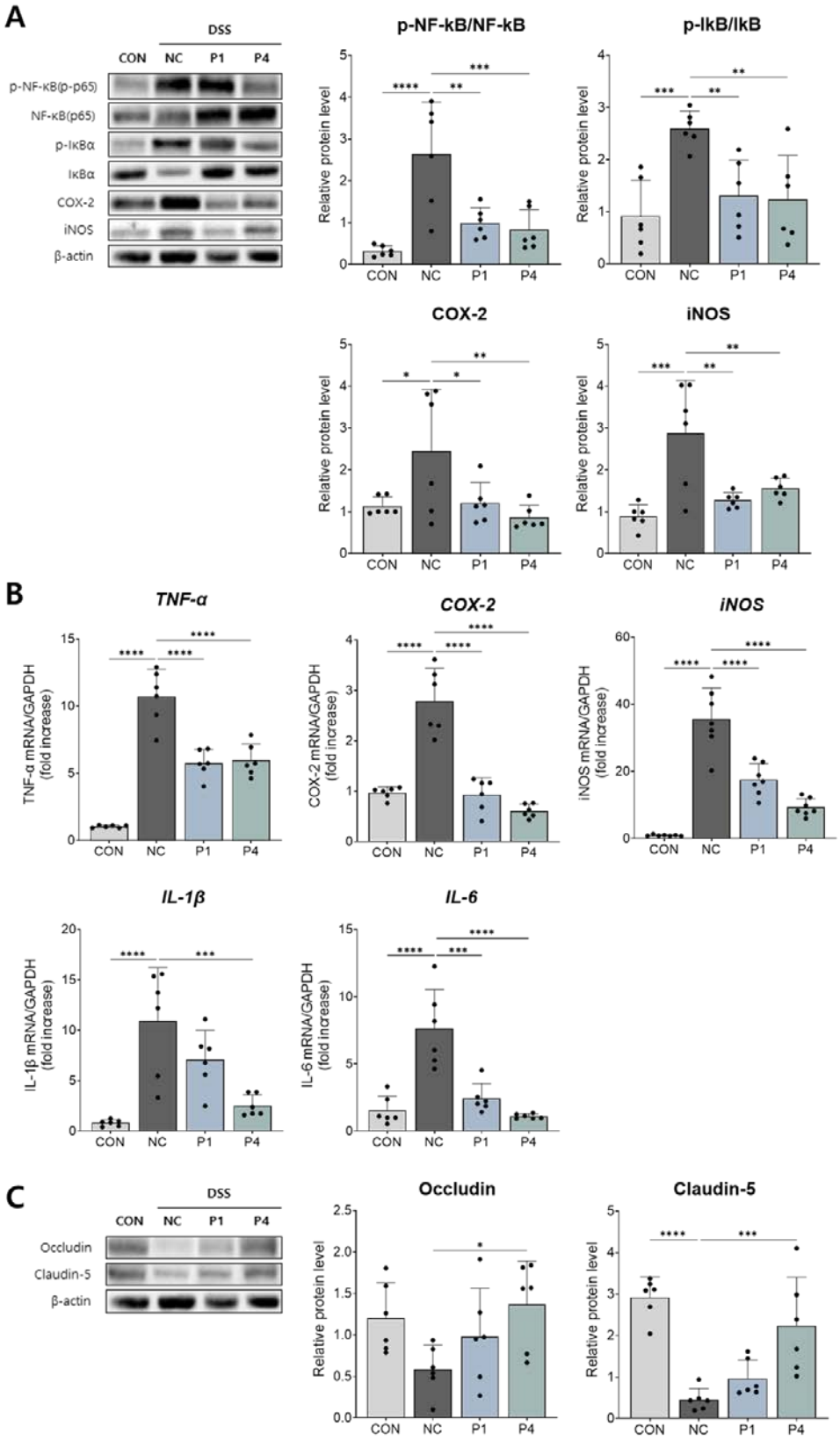



**Fig. 6 Effects of FSC-derived peptides on colonic inflammation and intestinal barrier function in DSS-induced colitis mice.** (A) Representative immunoblots and relative protein expression levels of p-NF-

κB/NF-κB, p-IκBα/IκBα, COX-2, and iNOS protein in colonic tissues determined by western blot. (B) Relative mRNA expression levels of *TNF-α*, *COX-2*, *iNOS*, *IL-1β*, and *IL-6* in colonic tissues. (C) Representative immunoblots and relative protein expression levels of tight junction proteins Occludin and Claudin-5 in colonic tissues determined by western blot. The p-NF-κB/NF-κB and p-IκBα/IκBα ratios were calculated relative to their corresponding total protein levels, whereas COX-2, iNOS, Occludin, and Claudin-5 protein levels were normalized to β-actin. mRNA levels were normalized to *GAPDH*, and relative mRNA expression is presented as $2^{-\Delta\Delta Ct}$. Statistical analysis of qRT-PCR data was performed on log2-transformed relative expression values. Data are presented as the mean ± SD (n = 6). Statistical significance was determined by one-way ANOVA followed by Šídák's multiple comparison test. *$p < 0.05$, **$p < 0.01$, ***$p < 0.001$, ****$p < 0.0001$.

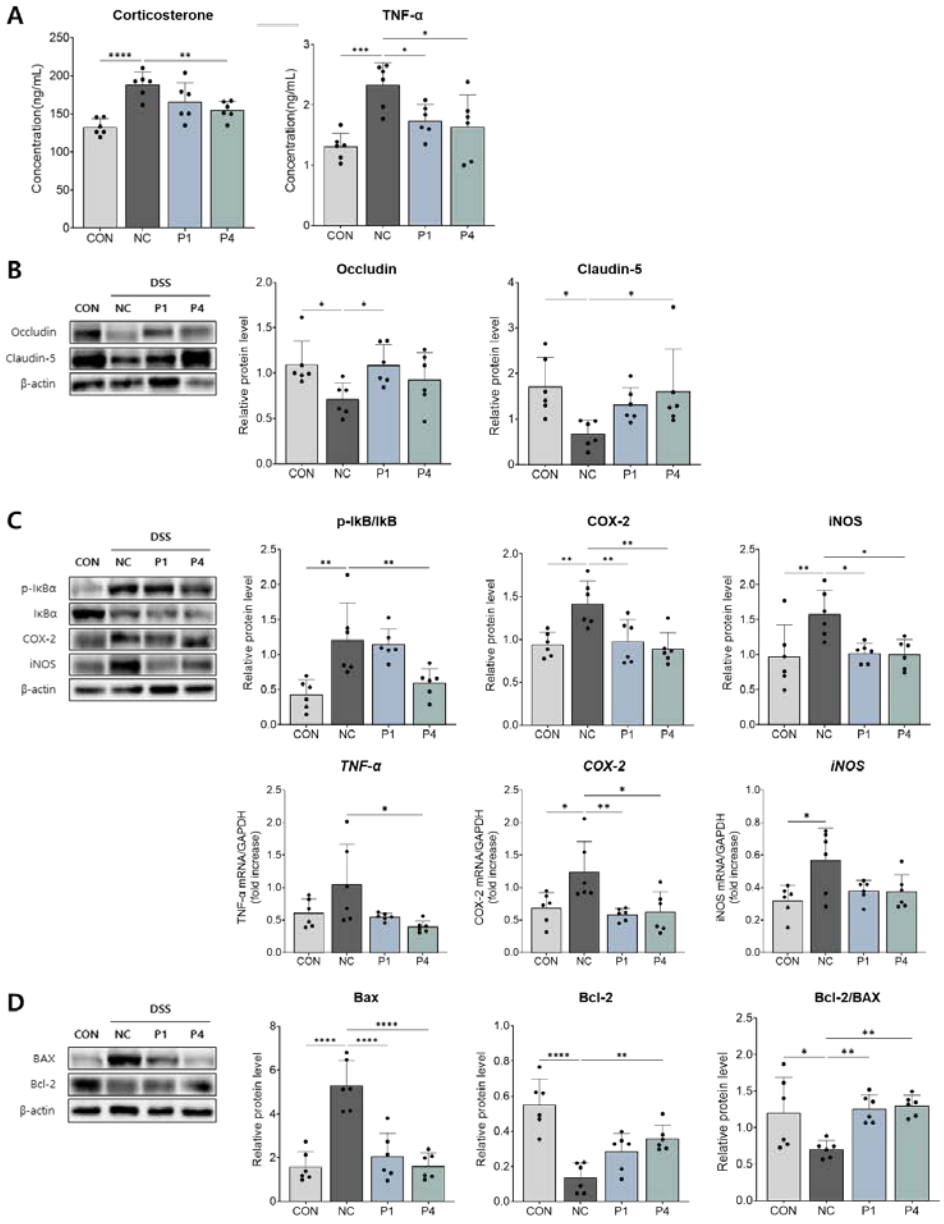



**Fig. 7 Effects of FSC-derived peptides on serum corticosterone and TNF-α levels, blood–brain barrier integrity, neuroinflammation, and neuronal apoptotic signaling in DSS-induced colitis mice.** (A) Serum corticosterone and TNF-α levels. (B) Representative immunoblots and relative protein expression levels of blood–brain barrier tight junction proteins Occludin and Claudin-5. (C) Representative immunoblots and quantitative analysis of p-IκBα/IκBα, COX-2, and iNOS protein expression, together with *TNF-α*, *COX-2*, and *iNOS* mRNA expression in brain tissues. (D) Representative immunoblots and relative protein expression levels of BAX and Bcl-2, together with the Bcl-2/BAX ratio, in brain tissues. The p-IκBα/IκBα ratio was calculated relative to total IκBα. COX-2, iNOS, Occludin, Claudin-5, BAX, and Bcl-2 protein levels were

normalized to β-actin, and the Bcl-2/BAX ratio was calculated using the corresponding β-actin-normalized values. mRNA levels were normalized to *GAPDH*, and relative mRNA expression is presented as $2^{-\Delta\Delta Ct}$. Statistical analysis of qRT-PCR data was performed on log2-transformed relative expression values. Data are presented as the mean ± SD (n = 6). Statistical significance was determined by one-way ANOVA followed by Šídák's multiple comparison test. *$p < 0.05$, **$p < 0.01$, ***$p < 0.001$, ****$p < 0.0001$.